IOP Conf. Series: Materials Science and Engineering **143** (2016) 012021 doi:10.1088/1757-899X/143/1/012021

Experimental study on directional solidification of Al-Si alloys under the influence of electric currents

D Räbiger, Y Zhang, V Galindo, S Franke, B Willers and S Eckert[1]

Helmholz-Zentrum Dresden-Rossendorf, 01314, Germany

E-mail: s.eckert@hzdr.de

Abstract. The application of electric currents during solidification can cause grain refinement in metallic alloys. However, the knowledge about the mechanisms underlying the decrease in grain size remains fragmentary. This study considers the solidification of Al-Si alloys under the influence of electric currents for the configuration of two parallel electrodes at the free surface. Solidification experiments were performed under the influence of both direct currents (DC) and rectangular electric current pulses (ECP). The interaction between the applied current and its own induced magnetic field causes a Lorentz force which produces an electro-vortex flow. Numerical simulations were conducted to calculate the Lorentz force, the Joule heating and the induced melt flow. The numerical predictions were confirmed by isothermal flow measurements in eutectic GaInSn. The results demonstrate that the grain refining effect observed in our experiments can be ascribed solely to the forced melt flow driven by the Lorentz force.

1. Introduction

The adjustment of fine grain morphologies is a crucial issue for improving characteristics and properties of cast and wrought aluminium alloys. Several methods are known to achieve grain refinement in solidification processes: add-on of grain refiners [1], rapid cooling conditions [2], mechanical or electromagnetic stirring [3], or ultrasonic treatment [4].

Grain refinement by inoculants is well reported as a very effective and well-known method which is widely used in foundry industry. It can be realized easily by addition of Al-Ti or Al-Ti-B master alloys and provides beneficial effects, for instance better feeding, reducing of hot tearing and improvement of strength [5,6]. However, the inoculation of the melt by grain refining particles may produce undesired side effects appearing as impurities or local defects in the microstructure. The electromagnetic treatment of solidifying alloys in form of electromagnetic stirring or the so-called Electric Current Pulse technique (ECP) unlocks a remarkable potential to influence the solidified macrostructure of metals during the solidification process. Many studies have shown that beneficial effects like a distinct grain refinement or the promotion of the transition from a columnar to an equiaxed dendritic growth (CET) can be achieved (see for instance [7-9]). However, the physical mechanism of the grain refinement effect caused by ECP has not been understood so far. Various effects are under discussion, such as the fragmentation of dendrite induced by the electric current [7], the reduction of the nucleation activation energy [8], or the break out and the transport of little grains from the boundary

[1] To whom any correspondence should be addressed.

by the periodic Lorentz force [9]. However, the possibility that intense Lorentz forces resulting from the interaction between the strong electrical current and the self-induced magnetic field can create significant melt flows was only insufficiently considered by previous studies. This situation was the motivation for us to perform an experimental study for investigating fluid flow effects during solidification of AlSi alloys under the impact of electric currents.

2. Experimental setup

Fig. 1(a) shows a schematic view of the experimental setup. A cylindrical vessel made of Perspex with an aspect ratio $A = H_0/2 \bullet R_0 = 1.2$ was used. The size of the inner diameter $D = 2 \bullet R_0$ and the filling height H_0 was chosen to be 50 mm and 60 mm, respectively. For fluid flow measurements the cylinder was filled with the eutectic alloy GaInSn. Two pencil electrodes (diameter 8 mm) are dipped through the free surface into the melt up to an immersion depth of 10 mm at opposite radial positions of $r_E = 18$ mm. The lateral surface of the electrodes is coated by an electrically insulating material in order to ensure that the electric current enters the liquid metal only through the front surface of the electrodes. The ultrasound Doppler velocimetry (UDV) was applied to measure the fluid flow inside the cylinder. More details about the measuring principle can be found in [10]. To achieve the acoustic coupling between sensor and fluid we attached the ultrasonic transducer to the bottom wall of the fluid container. A new measuring system of linear sensor arrays was used to realize a flow mapping of the meridional flow. Details of the measuring system are given in [11]. The spatial resolution in lateral direction varied from 5 mm at the sensor to approximately 7.5 mm at the lid of the fluid vessel. In axial direction a spatial resolution of about 1.5 mm was achieved. The velocity data were acquired with sampling frequencies between 0.5 and 6 Hz.

Solidification experiments were performed using an Al-7wt%Si alloy prepared from 99.99% Al and 99.999% Si according to the designated composition. The raw alloy was modified with 200ppm Sr. We give only a brief description here concerning the solidification experiment. Further details can be found in [12]. The Al-7wt%Si samples were solidified directionally from the bottom in a double-walled, cylindrical stainless steel mold. The mold has an internal diameter of 50 mm and a height of 100 mm. The schematic drawing of the experimental set-up can be found in Fig. 1(b). Preparatory specimens were made with a predetermined weight of 310 g corresponding to a filling height of 63 mm of the liquid in the mold. After melting the mold was positioned at a water-cooled copper chill which was kept at a constant temperature of about 20°C. In the experiments presented here the cooling of the sample and the influence of the electromagnetic field starts nearly at the same time.

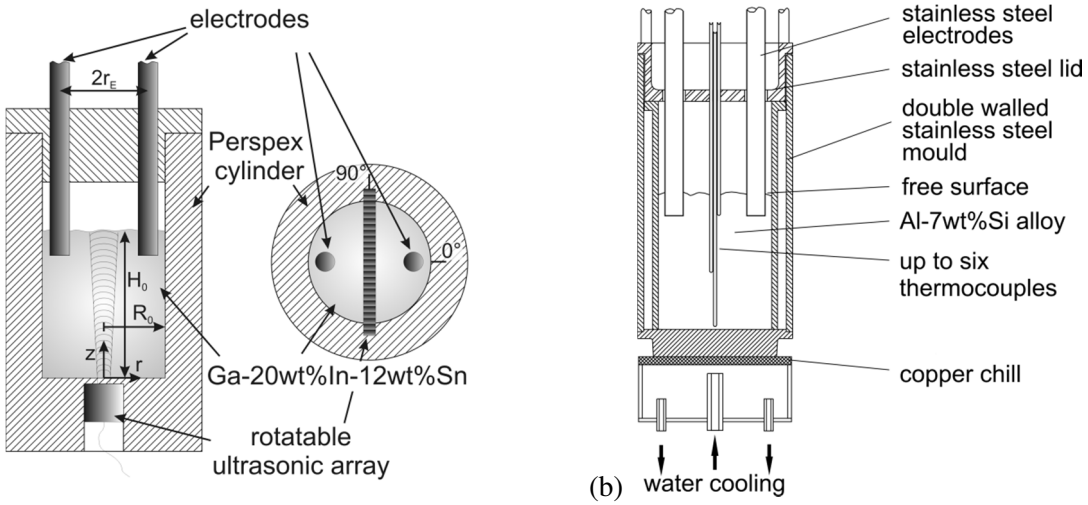

Figure 1. Schematic drawing of the experimental setup: (a) experimental setup for the fluid flow measurements, (b) experimental setup of the solidification experiments

To avoid an immediate formation of a solid shell the electrodes were preheated until achieving the same temperature as the melt before cooling from the bottom was initiated. The cables between the electrodes and the power supply were fixed at a considerable distance to the mold in order to minimize the interaction between the induced magnet field around the cable and the electric current flowing in the solidifying melt. The DC electric current and the current pulses are generated by the pulse reverse power supply pe86CWD (plating electronic). This device gives us the possibility to generate rectangular current pulses of variable pulse length at adjustable frequencies up to 200 Hz. Temperature measurements were made within the mold cavity during solidification using 6 type-K thermocouples arranged vertically along the axis of the mold. Temperature measurements were conducted at vertical positions of 1.5, 11, 22, 33, 44 and 55 mm above the bottom of the mold with an overall sampling rate of 5 Hz.

3. Numerical scheme

Numerical computations have been performed to calculate the actual distributions of electric current and magnetic field as well as the resulting Lorentz force. Furthermore, these simulations provide predictions of the flow field in the liquid metal column.

For the numerical simulations of the electric current $\boldsymbol{J}$ and the magnetic induction $\boldsymbol{B}$ in the melt and all electrically conducting parts of the facility the finite element code OPERA (Cobham plc. [13]) was used. In the case of a direct current imposed on the electrodes we solve the Laplace equation for the electric potential $\nabla^2 \varphi = 0$ taking into account the charge conservation and the continuity of the current density J at the interface between two regions with different electric conductivities: $J_n = -\sigma_1 \, \boldsymbol{n} \cdot \nabla \, \varphi_1 = -\sigma_2 \, \boldsymbol{n} \cdot \nabla \, \varphi_2$. The magnetic induction $\boldsymbol{B}$ was calculated from the current density $\boldsymbol{J} = \sigma \, (-\nabla \, \varphi)$ using the Biot-Savart law:

$$\boldsymbol{B}(\boldsymbol{r}) = \frac{\mu_0}{4\,\pi} \int d\,\boldsymbol{r}'^3 \, \frac{\boldsymbol{J}\,(\boldsymbol{r}') \times (\,\boldsymbol{r} - \boldsymbol{r}')}{|\,\boldsymbol{r} - \boldsymbol{r}'\,|^3} \tag{1}$$

The boundary conditions for the electric potential are defined using the amplitude of the imposed electric current at the end of the electrodes: $I_0 = \int_A \, d\,\boldsymbol{s} \cdot \boldsymbol{J}$, where A is the area of the electrode's cross section.

The flow in the volume containing the melt was simulated numerically by means of the open source library OpenFOAM [14] solving the Navier-Stokes equation together with the incompressibility condition and including an electromagnetic force density term:

$$\rho \left(\frac{\partial \, \boldsymbol{u}}{\partial \, t} + (\boldsymbol{u} \cdot \nabla) \, \boldsymbol{u} \right) = \, -\nabla \, p + \eta \, \nabla^2 \, \boldsymbol{u} + \boldsymbol{J} \times \boldsymbol{B} \tag{2}$$

The boundary conditions for the flow field are the no-slip condition $\boldsymbol{u} = \boldsymbol{0}$ at the solid container walls. For the melt surface either $\boldsymbol{u} = \boldsymbol{0}$ or the conditions for a stress-free, non-deformable surface $u_n = 0$ and $\partial \, u_t \, / \, \partial \, z = 0$ are applied depending on whether the melt flow is evaluated in an open or an enclosed container. A computational grid with 650000 volume elements was used.

In case of an applied alternating current the induced electromagnetic fields have to be taken into account. For that reason we used the force density term $\boldsymbol{f}_L = < \boldsymbol{J} \times \boldsymbol{B} >_T$ averaged over one period $T = 2\,\pi \, / \, \omega$.

The correct determination of the electromagnetic fields and the resulting Lorentz force density $\boldsymbol{f}_L = < \boldsymbol{J} \times \boldsymbol{B} >_T$ is an obvious prerequisite for the numerical simulation of the flow field.

4. Results

Parameter variations in case of a treatment with pulsed electric current concern the current amplitude I_P, the frequency f and the pulse length t_p. The pulse scheme is shown in figure 2(a). A first series of flow measurements were performed to investigate the impact of the current parameter on the fluid flow. Our flow measurements revealed that the global structure of the flow does not depend remarkably on the choice of parameter sets [15]. A typical flow field as predicted by numerical simulations is shown in figure 2(b). The melt flow is driven by a Lorentz force which is generated by the interaction between the radially diverging electric current at the tips of the electrodes and the almost azimuthally induced magnetic field. A strong downwards Lorentz force exists just below the electrodes, as shown in figure 2(c). This Lorentz force drives a flow in form of two descending jets. A recirculating flow occurs close to the cylinder walls within the lateral interspace on both sides of the electrodes. The numerical predictions are confirmed by corresponding flow measurements [15].

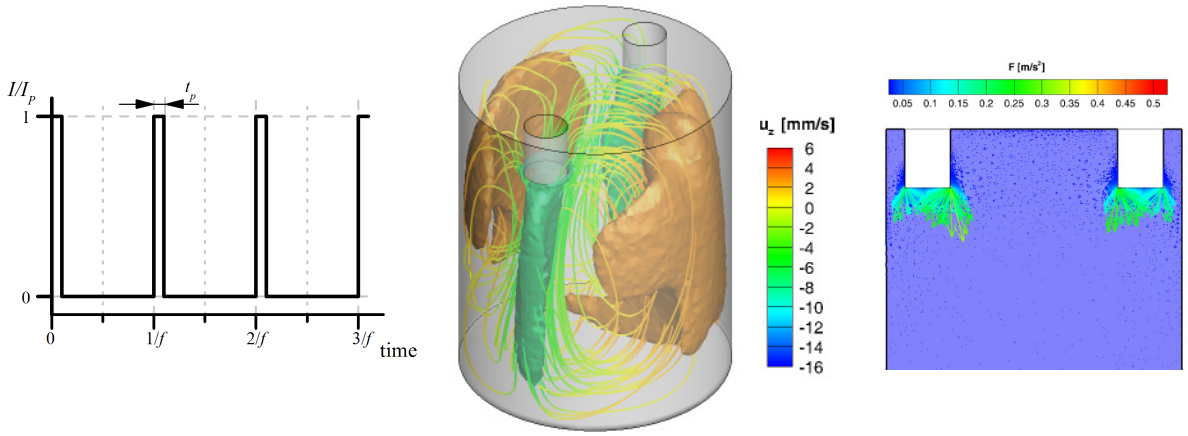

(a) (b) (c)

Figure 2. Schematic drawing of: (a) the pulse scheme, (b) numerical results showing the three-dimensional flow structure caused by the electric current and the interaction with the self-induced magnetic field (the iso-surfaces illustrate the vertical velocity, where negative and positive values represent an downward and upward flow, respectively) and (c) calculated Lorentz-force in the plane containing the electrodes

While the flow pattern remains similar for all parameter variations made here, the flow intensity is dependent on the parameters I_P, f and t_P. For comparison we introduce the effective value of the applied current amplitude $I_{eff} = I_P \cdot (t_P \cdot f)^{0.5}$. This value is equivalent with the energy input into the system. In the case of a direct current I_{eff} is equal to the applied I_{DC}.

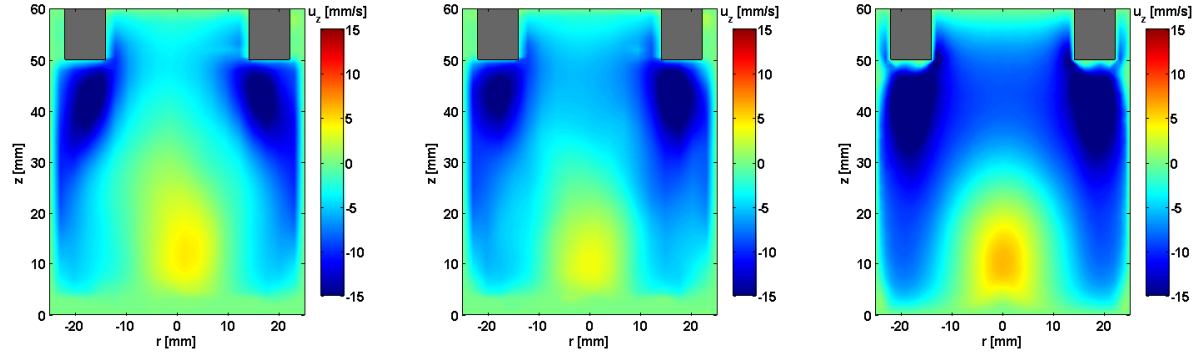

(a) (b) (c)

Figure 3. Two-dimensional distribution of the mean vertical velocity in the plane containing the electrodes measured at a) $I_{DC} = 48$ A, b) pulsed current with $I_P = 152$ A, $f = 200$ Hz, $t_P = 0.5$ ms ($I_{eff} = 48$ A) and c) numerical simulation with $I_{DC} = 48$ A

Figure 3(a) and (b) presents measurements of the averaged vertical velocity (u_z) recorded for a DC value of 48 A and a pulse current with I_{eff} = 48 A. The measurements show the flow structure in the plane containing the electrodes. However, the mean flow intensities and flow structure are almost identical. Figure 3(c) depicts the calculated results from the numeric with a DC current of 48 A. The general agreement of the numerical results is obviously. A more detailed picture of the flow structure and dynamic can be obtained in [16].

It is well-known from previous investigations, where the influence of melt stirring on solidification was studied, that the melt flow determines the temperature distribution in the sample. Figure 4(a) shows the evolution of the temperature along the sample axis at different vertical positions for different kinds of melt treatment. Figure 4(b) depicts the mean vertical temperature gradient averaged over the six measuring points along the axis. In case without any melt agitation (black line) we observe the development of an axial temperature gradient after the initiation of the cooling process. This temperature gradient is only slightly affected by applying electric current pulses at low effective currents (I_{eff} = 53.7 A – green line). An almost complete homogenization of the temperature field in the liquid phase is achieved by a further increase of the effective current (I_{eff} = 152 A – blue line). Distinct oscillations of the temperature signal indicate the occurrence of turbulent fluctuations in the liquid. Dendrite fragmentation by partial remelting can be promoted by the occurrence of such temperature and coupled solute fluctuations at the solidification front. This finding of a coupled temperature and solute fluctuation would be indirect affirmed by experiments in pure aluminium [17, 18]. The energy input caused by joule heating has no effect on the solidification time (achievement of solidus at the upper thermocouple (dashed line)). Figure 4 also contains a corresponding measurement obtained from a solidification experiment under the influence of electromagnetic stirring by a travelling magnetic field (TMF – red line). The field strength of the TMF (B_{TMF} = 12 mT) was chosen in such a way that the intensities of the generated melt flows (the mean intensity of the vertical velocities along the axis were taken as reference) can be expected to be almost the same.

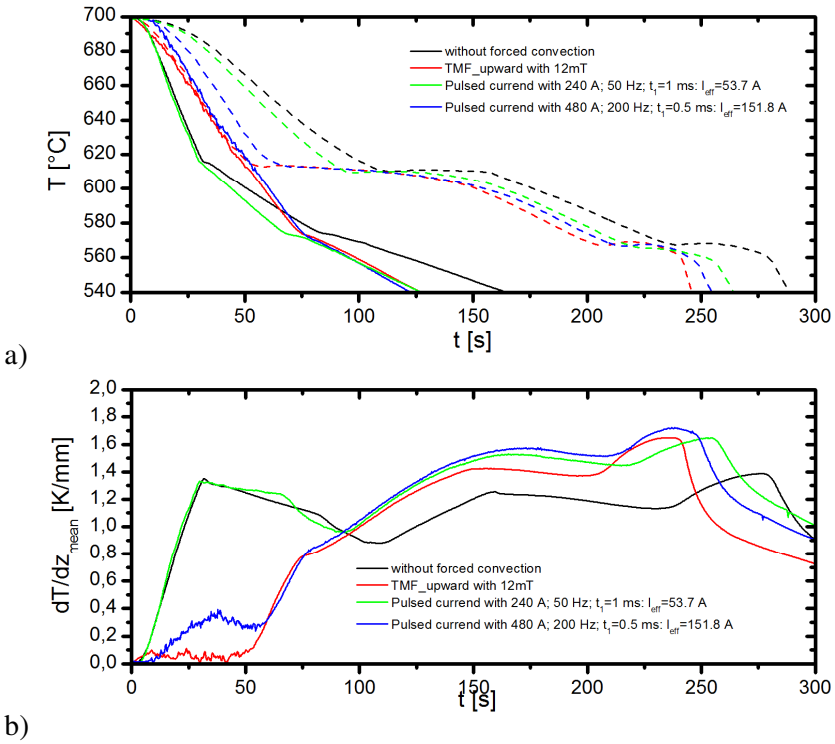

Figure 4. Measurements of the temperature along the sample axis during the solidification for varying kinds of melt forcing (a) for the vertical position z = 1.5 mm (solid line) and z = 55 mm (dashed line) and (b) the mean vertical temperature gradient averaged over six thermocouples

The TMF generates a flow pattern in form of a torus, where the melt flows downwards at the axis and upwards along the side walls of the cylinder [19, 20]. Thus, we can assume that the global flow structures driven by the TMF or the electric current in the experimental configuration considered here are not identical, but, rather similar.
The macrostructure of solidified samples in the longitudinal section is shown in figure 5. Coarse, columnar grains grow parallel to temperature gradient in the reference experiment without applied electric current (fig. 5(a)). A transition to an equiaxed structure of large grains occurs only just below the surface. The application of electric current pulses or a TMF changes the grain morphology completely. The section is covered by equiaxed grains which are significantly smaller as found for the untreated case. A few columnar grains still exist in the lower part of the sample which was processed under the influence of the electric current pulses (fig. 5(b)). It becomes obvious that these columnar dendrites are not perfectly aligned in vertical direction. It is known that the deflection of the columnar dendrites can be caused by a lateral incident flow [21, 22] or by an asymmetrical flow structure as shown in [23] for a TMF-driven flow where a small shift of the symmetry lines between magnetic field and mould axis caused significant changes of the flow structure. For our experiment we have to expect a slight asymmetry in the current-driven flow due to a non-symmetric configuration of the power lines around the experimental facility. This assumption is supported by the fact, that the measured flow field shows a deflection too, which change its direction if the electric current is applied with reversed polarity [16].

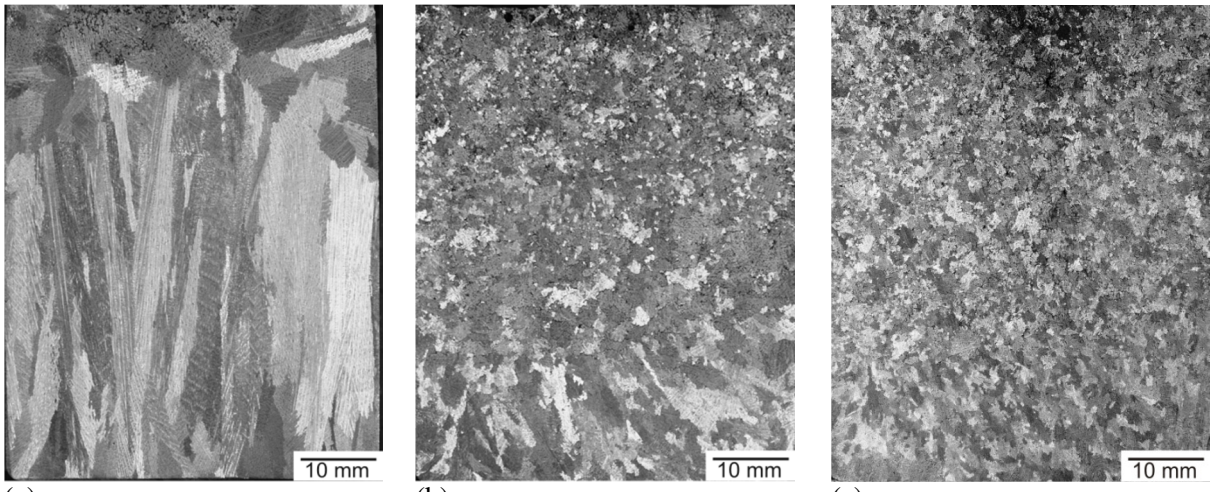

(a) (b) (c)

Figure 5. Macrostructure on the longitudinal section perpendicular to the plane containing the electrodes of the solidified samples: (a) without forced convection, (b) with I_{DC} = 152 A and (c) with downward TMF (B_{TMF} = 12 mT)

5. Conclusions

The present paper considers the impact of electric current on grain refinement in solidifying Al-Si alloys and the role of melt flow in this process. This so-called electro-vortex flow is driven by a Lorentz force caused by the interaction between the applied electric current and its own induced magnetic field. The flow intensity is determined by the time-averaged input of electric power which can be expressed by the effective current I_{eff}. A recent study revealed a reproducible correlation between I_{eff} and the grain size in the solidified samples, whereas the solidified structure becomes finer with increasing effective current. There are no remarkable differences with respect to the influence of a direct current or a treatment using electric current pulses on the mean grain size and the area of equiaxed zone in the solidified samples. The results demonstrate that the grain refining effect observed

in our experiments can be ascribed solely to the forced melt flow driven by the Lorentz force. A subsequent, systematic study is planned to investigate in detail the flow structure for other electrode configurations and a wide range of parameters. The results from this work will provide the basis for further research activities focusing on an optimization of the electric current treatment during solidification.

6. Acknowledgments

The research is supported by the German Helmholtz Association in form of the Helmholtz-Alliance "LIMTECH".

7. References

[1] McCartney DG 1989 Int. Mater. Rev. **34** 247
[2] Trivedi RK 1994 Mater. Sci. Eng. A **178** 129
[3] Flemings MC 1991 Metall. Trans. A **22** 957
[4] Eskin GJ 1998: Ultrasound treatment of Light Alloy Melt: Gordon and Breach, Amsterdam
[5] Murty BS, Kori SA and Chakraborty M 2002 Int. Mat. Rev. **47**(1) 3
[6] Quested TE 2004 Mater. Sci. Techn. **20** 1357
[7] Nakada M, Shiohara Y and Flemings MC 1990 ISIJ Int **30** 27
[8] Dolinsky Y and Elperin T 1993 Phys Rev B **47** 14778
[9] Li J, Ma JH, Gao YL and Zhai QJ 2008 Mater Sci Eng A **490** 452
[10] Takeda Y 1991 Nucl. Eng. Design **126** 277
[11] Franke S, Lieske H, Fischer A, Büttner L, Czarske J, Räbiger D, Eckert S 2013 Ultrasonics **53** Issue 3 691
[12] Willers B, Eckert S, Nikrityuk PA, Räbiger D, Dong J, Eckert K and Gerbeth G 2008 Metall. Mater. Trans. **B 39** 304
[13] http://www.comham.com/emdesign
[14] http://www.openfoam.org
[15] Räbiger D, Zhang Y, Galindo V, Franke S, Willers B and Eckert S 2014 Acta Mater. **79** 327
[16] Franke S, Räbiger D, Galindo V, Zhang Y and Eckert S 2015 Flow Meas Inst in press
[17] Edry I, Erukhimovitch V, Shoihet A, Mordekovitz Y, Frage N and Hayun S 2013 J Mater Sci **48** 8438
[18] Zhang Y, Räbiger D, Eckert S 2016 J Mater Sci **51** 2153
[19] Cramer A, Zhang C, Eckert S 2004 Flow Meas Instrum 2004 **15** 145
[20] Metan V, Eigenfeld K, Räbiger D, Eckert S 2009 J Alloy Compnds **487** 163
[21] Eckert S, Willers B, Nikrityuk P A, Eckert K, Michel U and Zouhar G 2005 Mater Sci. Eng. **A413-414** 211
[22] Eckert S, Räbiger D, Matthes M, Zimmermann G, Schaberger-Zimmermann E 2012 IOP Conference Series: Materials Science and Engineering **27** 012051
[23] Cramer A, Pal J, Koal K, Tschisgale S, Stiller J, Gerbeth G 2011 J of Crystal Growth **321** 142